Neutronic Feasibility of a Breakeven Molten Salt Fast Reactor Starting with HALEU

Eunhyug Lee [a], Taesuk Oh [a], Ji Hwan Kim [b], and Yonghee Kim [a*]
[a] *Korea Advanced Institute of Science and Technology, 291 Daehak-ro, Yuseong-gu, Daejeon 34141, Republic of Korea*
[b] *Hyundai Engineering & Construction, 75, Yulgok-ro, Jongno-gu, Seoul, 03058, Republic of Korea*
[*] *Corresponding author: yongheekim@kaist.ac.kr*

Keywords : Breakeven molten salt fast reactor (BeMFR), hybrid chloride-fluoride salt, closed fuel cycle, HALEU, Monte Carlo

1. Introduction

Growing environmental pressures and the demand for reliable energy supply have renewed global interest in nuclear power as an alternative to fossil fuels [1]. Nonetheless, the long-term deployment of nuclear energy is constrained by three critical issues: ensuring a higher level of reactor safety, managing the accumulation of spent nuclear fuel, and securing adequate uranium resources. Conventional LWRs make only limited use of natural uranium, and the declining availability of storage capacity for spent fuel further undermines their sustainability. One potential solution is to recycle spent fuel as a secondary resource, a strategy that could be realized through the advancement of next-generation reactor systems.

Prior studies have investigated the implementation of a closed fuel cycle in conjunction with molten salt fast reactors (MSFRs) to address key challenges in nuclear energy, emphasizing advantages such as enhanced passive safety [2], reduced accumulation of spent fuel, and improved proliferation resistance. Within this framework, a breakeven molten salt fast reactor (BeMFR) aims to balance the production and consumption of fissile material, thereby enabling sustainable reactor operation. Previous BeMFR concepts [3-4] employed TRU as the initial fuel, prepared through simplified pyro-processing, successfully demonstrating breakeven operation. Although this approach offers strong proliferation resistance, immediate access to spent fuel may be restricted depending on national regulations. To overcome this limitation, the present study investigates the use of high-assay low-enriched uranium (HALEU) as the initial fissile material for BeMFRs and evaluates the potential for long-term, sustainable operation.

2. Fuel Cycle and Reactor Model

2.1 Fuel Cycle

Figure 1 illustrates a closed fuel cycle concept based on a HALEU-fueled BeMFR. In this configuration, a breakeven state is sustained through the continuous removal of fission products (FPs) and the addition of make-up fuel. Noble gases are separated, for instance, by helium sparging; economically valuable elements such as Pd and Nd can be recovered for reuse; whereas highly radiotoxic isotopes including Cs and Sr must be directed to dedicated storage. Initial criticality is achieved with HALEU, after which the core is refueled using spent nuclear fuel from LWRs, treated via reduction and chlorination. During this treatment, most fission products are eliminated from the spent fuel, with the exception of rare earth elements.

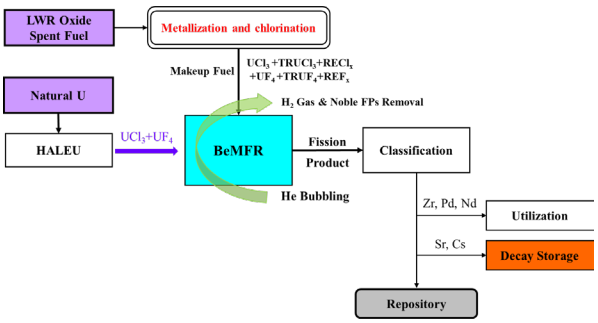

Fig. 1. Closed fuel cycle based on the BeMFR starting with HALEU

2.2 Fuel and Reactor Model

As noted previously, reduction and chlorination processes selectively remove non-rare-earth fission products. The resulting treated spent fuel serves as make-up material for sustaining the criticality of the BeMFR. The detailed composition of this processed fuel is provided in Table I [3].

Table I: Spent fuel composition after removing non-RE fission products

Element	Mass fraction [%]	Element	Mass fraction [%]	Element	Mass fraction [%]
Y	5.122E-04	Eu	2.129E-04	Th	1.307E-09
La	1.797E-03	Gd	4.361E-04	Pa	2.430E-11
Ce	3.486E-03	Tb	7.060E-06	U	9.718E-01
Pr	1.618E-03	Dy	3.658E-06	Np	4.530E-04
Nd	5.925E-03	Ho	4.905E-07	Pu	1.120E-02
Pm	1.280E-05	Er	2.090E-07	Am	1.106E-03
Sm	1.209E-03	Tm	1.246E-09	Cm	2.625E-04

To secure a sufficient uranium fraction, this study employs a chloride–fluoride hybrid fuel. Figure 2 presents the phase diagram of the KCl-UCl_3-UF_4 ternary system [5], hereafter referred to as the chloride-fluoride hybrid salt. At the eutectic composition of 28wt.%-

36wt.%-36wt.%, this salt exhibits a melting point of approximately 475 °C.

Two cases are considered: Case A, which assumes pure uranium, and Case B, which incorporates uranium with a representative fraction of rare earth (RE) elements. For Case B, the KCl fraction is fixed at 28%, while the remaining portion is equally divided between chlorides (UCl_3, $RECl_3$) and fluorides (UF_4, REF_4). The RE distribution is assumed to match that of the spent nuclear fuel (SNF) composition provided in Table I.

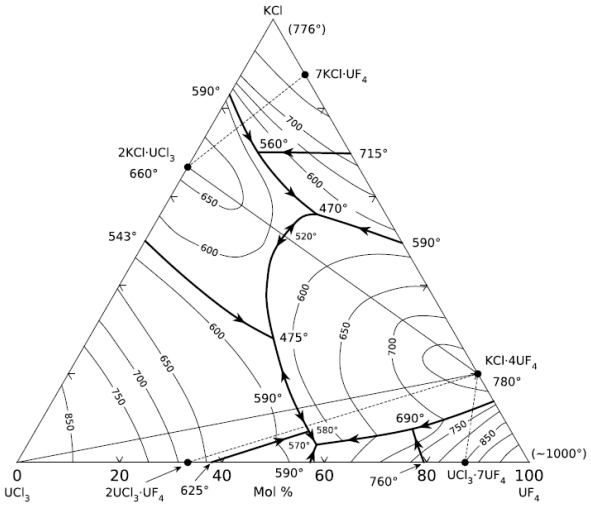

Fig. 2. Phase diagram of KCl-UCl_3-UF_4 [5]

Simplified BeMFR configuration for Cases A and B were modeled. Reactor shape is a cylindrical core as illustrated in Figure 3. The active region, containing liquid fuel, is encased by a stainless-steel reflector to improve neutron economy. Beyond the reflector, a heat exchanger connected to the active core enables the circulation of molten salt fuel between the core and the secondary system. Reactivity control mechanisms are also incorporated within the reflector. The active core is designed with both diameter and height fixed at 300 cm. For both models, the inactive salt volume is assumed to be 15 m³. Each reactor is operated at a thermal power of 3,000 MWth, with additional design specifications summarized in Table II.

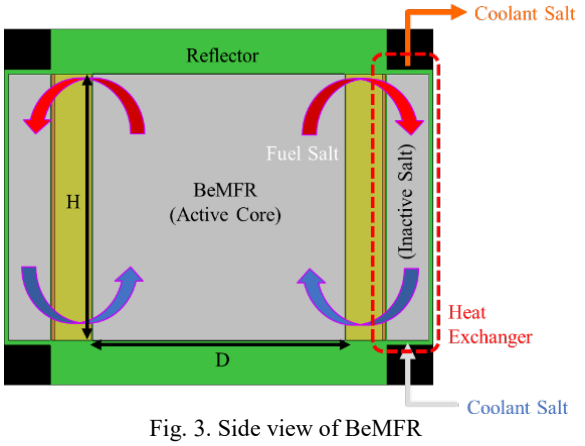

Fig. 3. Side view of BeMFR

Table II: Design parameter of initial BeMFRs

	Case A	Case B
Power	3,000 MWth	3,000 MWth
Initial molar composition of KCl-UCl_3-$RECl_3$-UF_4-REF_4	28-36-0-36-0	28-34-2-34-2
Uranium enrichment	19.75 wt.%	19.75 wt.%
Density (650°C)	4.768 g/cm³	4.696 g/cm³
Diameter	300 cm	300 cm
Height	300 cm	300 cm
Active core volume	2.121E+7 cm³	2.121E+7 cm³
Inactive salt volume	1.500E+7 cm³	1.500E+7 cm³
U mass	113,762 kg	107,422 kg
RE mass	0 kg	3,739 kg
Average fuel temperature	923.15 K	923.15 K
Pressure of the system	1 atm	1 atm

3. Numerical Results

This section is to examine the feasibility of BeMFR using HALEU. The outlined operational strategies include make-up fuel feeding and FP removal. Simulations were performed using the Monte Carlo–based Serpent 2.2.1 code with the ENDF/B-VII.1 nuclear data library.

In molten salt reactors (MSRs), fission products (FPs) are generally categorized into noble gases, noble metals, and soluble species according to their chemical behavior. Noble gases are released in gaseous form, noble metals remain insoluble and precipitate from the molten salt, while soluble FPs are retained in the salt phase. The representative elements belonging to each category are listed in Table III.

Table III: Design parameter of initial BeMFR [6]

Noble gas	Kr, Xe, Rn
Noble metal	Co, Ni, Cu, Ge, As, Se, Mo, Tc, Ru, Rh, Pd, Ag, Sn, Sb, Te, W, Re, Os, Ir, Au, Hg, Bi, Po
Soluble FP	Cr, Mn, Fe, Zn, Ga, Br, Rb, Sr, Y, Zr, Nb, Cd, In, I, Cs, Ba, La, Ce, Pr, Nd, Pm, Sm, Eu, Gd, Tb, Dy, Ho, Er, Tm, Yb, Lu, Hf, Ta, Pt, Tl, Pb, At, Fr, Ra

To accurately represent the behavior of noble gases subject to rapid removal and to account for hydrogen extraction, the noble gas removal rate is set at 1% per second, while hydrogen is removed at a rate of 90% per year. The noble metal removal rate is assumed to be 60% annually. These parameters are applied consistently across all operational periods, as summarized in Table IV.

Table IV: Reactor operation strategy (common)

Noble gas removal rate	1 %/s
Noble metal removal rate	60 %/y
Hydrogen removal rate	90 %/y

Operational strategies such as the soluble FP removal rate, make-up fuel supply rate, and RE feeding rate differ depending on the case and the stage of operation. These parameters are illustrated in Figs. 4 and 5. Figure 4

presents the soluble FP removal rates for Cases A and B, while Fig. 5 shows the make-up fuel and RE feeding rates. A comparison between the two cases indicates that the presence of RE in the initial core increases the maximum soluble FP removal rate, which is estimated to be 2.6%/y for Case A and 6.0%/y for Case B. As shown in Fig. 5, Case A requires an additional RE feed during part of the operation, whereas in Case B, there exists a period where no makeup or RE feedings are necessary.

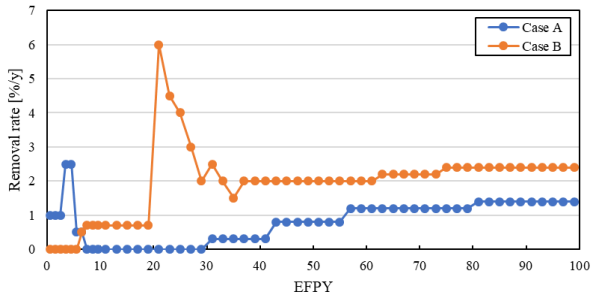

Fig. 4. Soluble FP removal rates

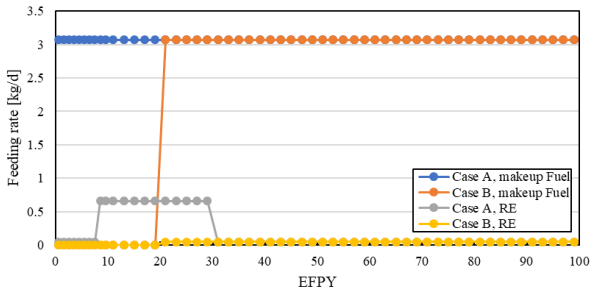

Fig. 5. Make-up fuel and RE feeding rates

Figure 6 presents the calculated variations in reactivity and the effective delayed neutron fraction (β), while Fig. 7 shows the conversion ratio. Reactivity fluctuations are observed during the transitional stages; however, these gradually diminish toward the end of the operation, leading to convergence in both reactivity and conversion ratio. It may be inferred that subdividing the operational periods and optimizing the fission product removal rates can markedly reduce, or even nearly eliminate, such fluctuations. Under these conditions, reactivity stabilizes around 400 pcm. The effective delayed neutron fraction decreases from approximately 700 pcm to about 400 pcm, reflecting fuel conversion. In Case A, there is an interval during which reactivity temporarily exceeds 1 $, whereas in Case B, the reactivity does not rise significantly above this threshold. The conversion ratio begins at about 0.85–0.8 and eventually increases to approximately 1.03.

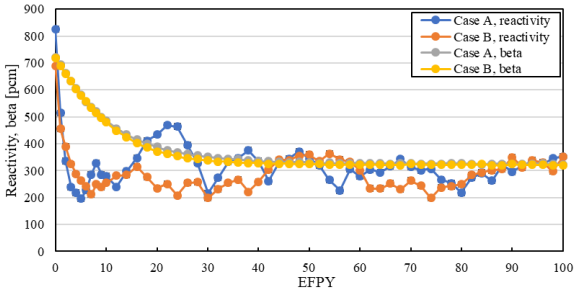

Fig. 6. Reactivity, beta evolutions

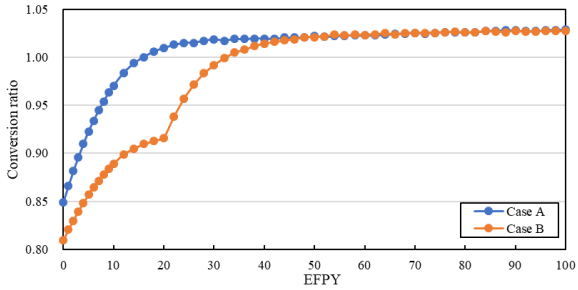

Fig. 7. Conversion ratios

Figure 8 illustrates the temporal variation of fuel volume throughout reactor operation. In Case A, where no RE is initially included, the continuous buildup of fission products leads to a pronounced increase in total fuel volume. This excessive swelling may exceed the design limits of the core, posing potential challenges to both fuel accommodation and system integrity. By contrast, Case B, which assumes partial inclusion of RE at the start of operation, significantly alleviates this problem by moderating the extent of fission product accumulation. The numerical results highlight this distinction: in Case A, the fuel volume increases by more than 40% relative to the initial state, while in Case B the variation remains confined within a relatively small window of approximately –3% to +7%. This comparison suggests that incorporating RE in the initial fuel composition can serve as an effective strategy to stabilize fuel volume and ensure the operational feasibility of the BeMFR.

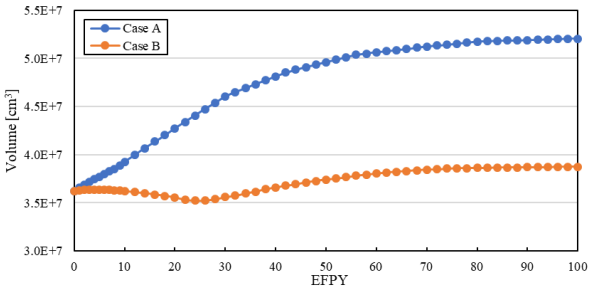

Fig. 8. Evolutions of fuel volumes

Figure 9 depicts the temporal evolution of U-235 and Pu-239 masses during reactor operation. At the beginning, U-235 serves as the dominant fissile isotope driving the chain reaction. However, its inventory steadily decreases over time, eventually becoming a minor contributor to the overall fission process. In

contrast, Pu-239 is absent in the initial core but is continuously bred from U-238, leading to a gradual increase in its inventory. As operation progresses, Pu-239 accumulates until it approaches an equilibrium level, at which point it becomes the principal fissile species sustaining criticality. Once the rates of Pu-239 production, consumption, and refueling are balanced, both the system reactivity and the Pu-239 inventory stabilize. At equilibrium, the Pu-239 masses are calculated to be approximately 12.6 tons for Case A and 9.6 tons for Case B, respectively.

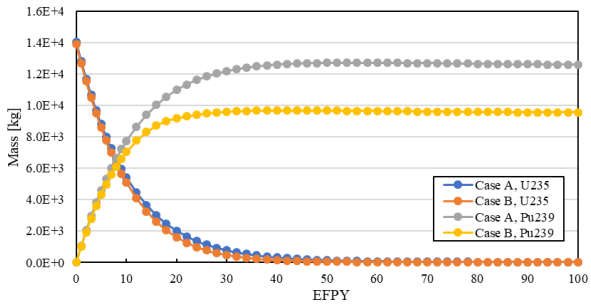

Fig. 9. U-235 and Pu-239 mass evolutions

4. Conclusions

This study demonstrates the feasibility of using HALEU as the initial fissile material in breakeven molten salt fast reactors (BeMFRs), offering an alternative to TRU-based fueling strategies. By integrating a closed fuel cycle with molten salt fast reactor technology, sustainable operation can be achieved while maintaining high proliferation resistance, mitigating spent fuel accumulation, and enhancing reactor safety. The analysis shows that HALEU can successfully initiate criticality and support long-term operation, even when immediate access to spent fuel is limited. These results indicate that HALEU-fueled BeMFRs provide a viable approach to sustainable and resilient nuclear energy, addressing both resource utilization and safety challenges associated with conventional light-water reactors. Further investigations into fuel cycle optimization and experimental validation of operational parameters are essential to advance this concept toward practical deployment.

Acknowledgments

This research was supported by the KAIST Convergence Research Institute Operation Program and Korea Energy Technology Evaluation and Planning (KETEP) grant funded by the Korean Government (MTIE) (RS-2024-00439210), and the National Research Foundation of Korea (NRF) grant funded by the Korean Government (MSIP) (2021M2D2A207638322).

REFERENCES

[1] L. Liu, H. Guo, L. Dai, M. Liu, Y. Xiao, T. Cong, & H. Gu (2023). The role of nuclear energy in the carbon neutrality goal. Progress in Nuclear Energy, 162, 104772.
[2] D. E. Holcomb, G. F. Flanagan, B. W. Patton, J. C. Gehin, R. L. Howard, & T. J. Harrison (2011). Fast spectrum molten salt reactor options. ORNL/TM-2011/105.
[3] E. Lee, T. Oh, & Y. Kim, Neutronic Feasibility of a Breakeven Molten Salt Fast Reactor Using a Hybrid Chloride-Fluoride Salt, Transactions of the Korean Nuclear Society Spring Meeting, Jeju, Korea, May 22-23, 2025
[4] E. Lee, T. Oh, & Y. Kim, Neutronic Feasibility of Breakeven Molten Salt Fast Reactor Based on a Closed Fuel Cycle, Transactions of the American Nuclear Society Annual Conference, June 15–18, 2025, Chicago, IL
[5] V. N. Desyatnik, et al. "Phase diagram of the KCl-UCl3-UF4 system." Izvestiya Vysshikh Uchebnykh Zavedenij. Tsvetnaya Metallurgiya (1973, Soviet Union): 132-134
[6] S. Yoon, J. W. Park, H. Eun, & J. Yun, Estimating the electroneutrality of fission products in molten chloride fast reactor. Korean Radioactive Waste Society 2024 Autumn Conference, Gyeongju, Korea, October 30 – November 1, 2024